

# Dual band tunable absorber with graphene in THz range

ZHAO HONG-LIANG, REN GUANG-JUN\*, CHEN ZHI-HONG\*\*, LIU FEI, XIN HUAN-PENG

School of Electrical and Electronic Engineering; Tianjin Key Lab. of Film Electronic & Communication Devices; Engineering Research Center of Communication Devices and Technology, Ministry of Education; Tianjin University of Technology; Tianjin 300384, PR China

A dual band perfect tunable graphene absorber in the terahertz range is proposed in this paper. The unit cell of the structure consists of symmetric graphene strips and a silicon layer deposited on a gold film. The structure shows a very high absorbance of 98.3% and 98.7% at 3.54THz and 5.12THz in simulations, respectively. Both the resonance wavelengths of the absorber blue shift with the increase in Fermi level of graphene. Moreover, the surface current distributions on the graphene resonator at the two resonance wavelengths are simulated to deeply understand the physical mechanism of resonance absorption. The absorber offers a new way for the applications in the terahertz range.

(Received May 4, 2016; accepted April 6, 2017)

*Keywords:* Graphene, Tunable, Absorber, Terahertz

## 1. Introduction

Recently, terahertz technology has become more and more mature. Metamaterial-based devices, such as absorbers [1], filters [2] and modulators [3]. The metamaterial absorber is the typical device in terahertz range. Absorber has potential application such as micro bolometers, spectrum imaging, optical detectors, stealth technology, etc. At the beginning, modulation method of absorber merely modulates intensity of absorption or resonant frequency. Nowadays wide bandwidth and multiband absorber have emerged. But in the future we require above properties all in one.

Graphene as a new two-dimensional metamaterial, with a high electron mobility. The conductivity can be adjusted by doping or bias voltage, so it is possible to fabricate tunable absorber. In recent years, the devices based on graphene have attracted many attentions, such as sensors [4] and dual-band absorber [5,6].

## 2. Design and simulation

The general pattern of absorber is shown in Fig. 1(a), it's a periodic array structure with graphene on top layer and silicon deposited on the metal layer. The Schematic of unit is shown in Fig. 1(b), where  $h$  is silicon thickness and the structure parameters are shown in Table 1. THz wave cannot penetrate the gold layer thicker than 100nm, so the absorption is simply expressed as  $A = 1 - R$ , where  $R$  is the reflection.

Table 1. Structural parameters of two peaks tunable absorber (unit:  $\mu\text{m}$ )

$a$	$b$	$d$	$h$	$L$	$t_{\text{gold}}$
1.00	0.30	0.05	4.30	2.00	0.20

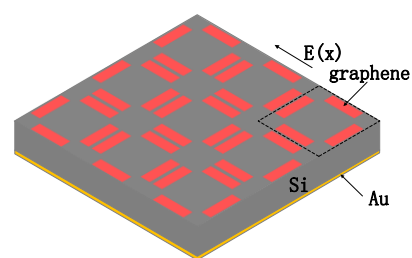


Fig. 1(a). Schematic of the graphene strips perfect absorber

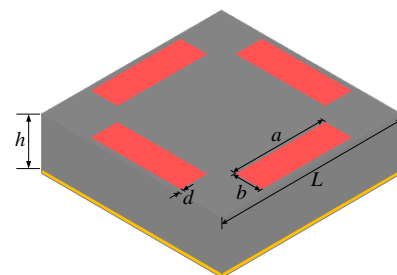


Fig. 1(b). Schematic of a unit

The complex surface conductivity of graphene is given by Kubo formula [7], which is:

$$\sigma_g^{total} = \sigma_g^{intra} + \sigma_g^{inter} = \frac{ie^2k_B T}{\pi\hbar^2(\omega+i2\Gamma)} \left\{ \frac{E_F}{k_B T} + 2 \ln[\exp(-E_F/k_B T) + 1] \right\} + \frac{ie^2}{4\pi\hbar} \ln \left[ \frac{2|E_F| - (\omega+i2\Gamma)\hbar}{2|E_F| + (\omega+i2\Gamma)\hbar} \right] \quad (1)$$

In this formula, conductivity of graphene contains intraband and interband transitions, where  $\Gamma$  is the scattering rate ( $2\Gamma = \hbar/\tau$ ,  $\tau$  is the electron-phonon relaxation time),  $k_B$  is The Boltzmann's constant,  $\omega$  is the radian frequency,  $T$  is the room temperature fixed to 300K,  $\hbar$  is reduced Planck's constant,  $E_F$  is the Fermi level and  $e$  is the charge of an electron. In the low terahertz range, the contribution of interband transition to surface conductivity can be neglected compared to the intraband transition. Then the conductivity of graphene can be approximately described by Drude model [7,8,9]. For  $k_B T \ll E_F$ , Eq. (1) can be simplified as [8,9,10,11]:

$$\sigma_g^{total} \approx \frac{e^2 E_F}{\pi\hbar^2} \frac{i}{\omega + i\tau^{-1}} \quad (2)$$

As mentioned above, the conductivity can be controlled by adjusting  $E_F$ , the shift of resonance spectrum is determined by the imaginary part of the conductivity, the amplitude of resonance modulation depends on the real part of the conductivity. So the absorption intensity can be adjusted by the variation of conductivity of graphene. In this paper, we applied an external electric field to change  $E_F$ , the direction along  $x$  axis as shown in Fig. 1(a). In Fig. 2, we demonstrate the numerical simulation of the imaginary part conductivity and the real part conductivity of the single layer graphene with different  $E_F$ , respectively.

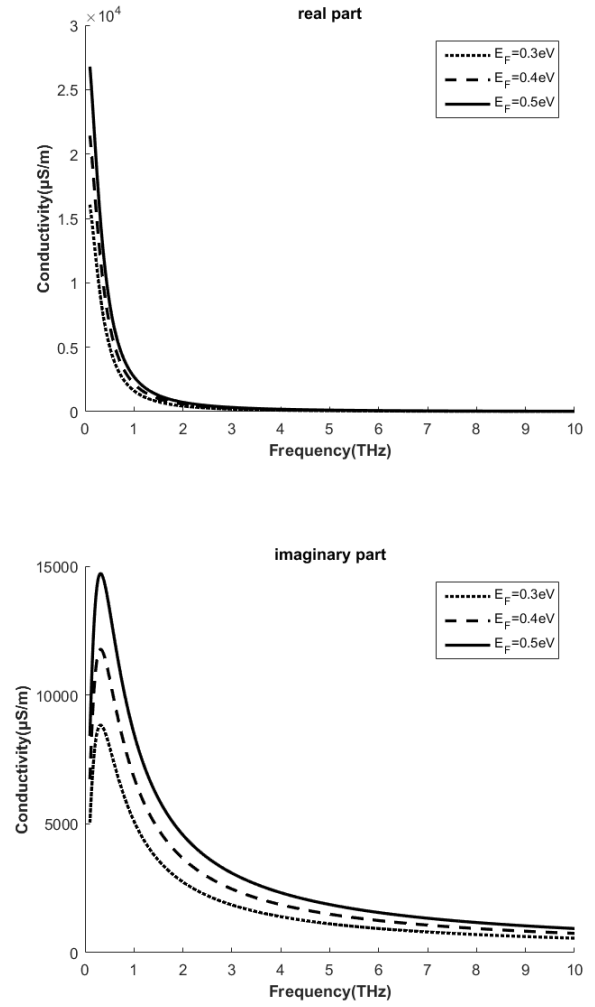


Fig. 2. Graphene conductivity

### 3. Results

The  $xy$  plane of unit shows in Fig. 3(a), we set the four graphene parts as  $g_1$ ,  $g_2$ ,  $g_3$ ,  $g_4$ , respectively. Then we simulated when there existed only  $g_1$ ,  $g_2$  (Specified as P1) or  $g_3$ ,  $g_4$  (Specified as P2) on the silicon substrate, with  $E_F = 0.5eV$  and  $\Gamma = 0.5meV$ . In Fig. 3(b), it shows dual band absorber as P (solid line), P1 (dotted line) and P2 (dashed line). In the P structure, the absorption of them achieves 98.3% and 98.7% at 3.54THz and 5.12THz, respectively. The physical explanation stems from the electric resonance in the graphene strips owing to localized surface plasmon resonance and the magnetic resonance [12] between the graphene strips array and gold film.

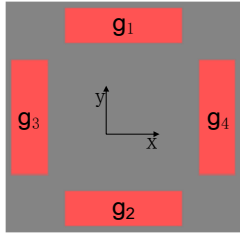


Fig. 3(a). Schematic of the  $xoy$

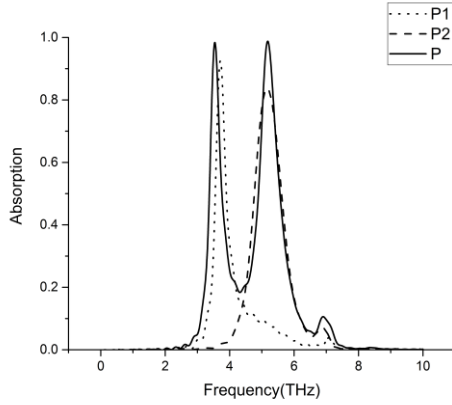


Fig. 3(b). The absorption spectra of structure

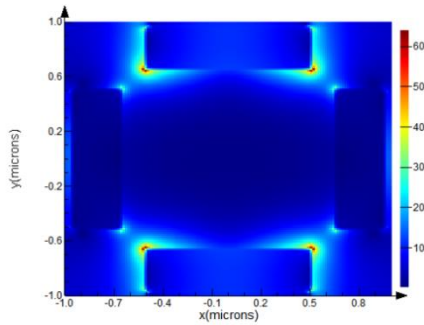


Fig. 3(c). The electric field distribution on the graphene strips of unit cell at 3.54THz

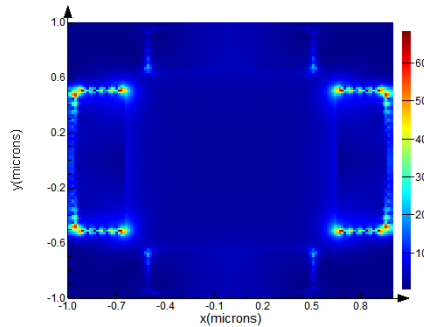


Fig. 3(d). The electric field distribution on the graphene strips of unit cell at 5.12THz

#### 4. Discussions

Due to the effect of incident wave, opposite charge will be assembled in the two ends of the graphene strips [12]. As shown in Fig. 3(c) and Fig. 3(d) at 3.54THz and 5.12THz, respectively. Electric resonance is formed in the graphene strips. Then the induced electric resonance and the bottom gold film generate a coupling effect. We find that Fig. 3(c) is the quadrupole resonance and Fig. 3(d) is the dipole resonance. Due to the charges are confined to the ends of the strips, so we assume that the electric field is distributed at the two ends of the strips, and the distribution of the surface current as shown in Fig. 4(a) and Fig. 4(b) at 3.54THz and 5.12THz, respectively. In Fig. 4(a) and Fig. 4(b) we can clearly observe the electric field generated by the electric resonance. Moreover, the charge distribution in graphene strips leads to the opposite charge distribution on the gold film and exerts the magnetic resonance. As Fig. 3(b) shown, it appears two resonance absorption peaks.

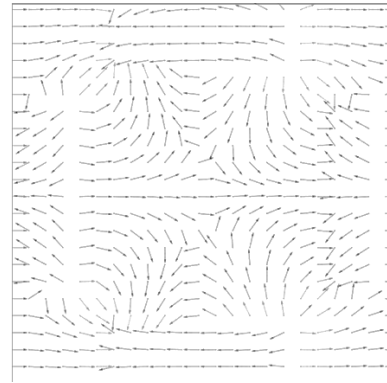


Fig. 4(a). Distributions of surface current on graphene strips at 3.54THz

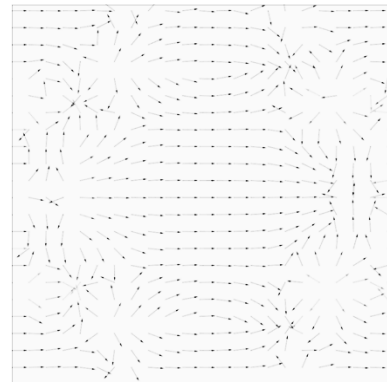


Fig. 4(b). Distributions of surface current on graphene strips at 5.12THz

The performance of polarization sensitive of metamaterial absorber was investigated under our work. As shown in Fig. 5, the two dark regions show that absorbance in both bands remains strong from 0 to 50

degrees. Due to the symmetric structure, the absorber is nearly insensitive to polarization.

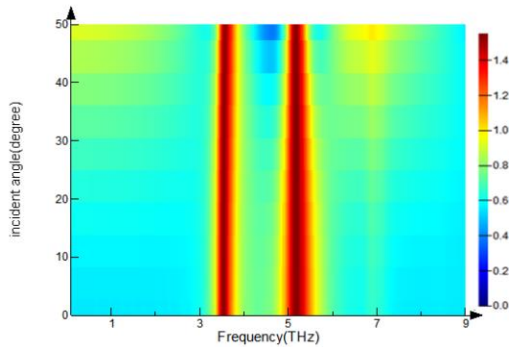


Fig. 5. Absorbance spectrum as a function of frequency and incident angle

As shown in Fig. 2, the surface conductivity of graphene is closely related to the Fermi level. We have a numerical calculation of the absorption for different values of  $E_F$  at normal incidence as shown in Fig. 6. Blue shifts of absorption were observed when the  $E_F$  from  $0.3eV$  to  $0.6eV$  with an obvious absorption gain. The change in absorption can be comprehended as a simplified reason, the size of the structure is much smaller than the incident wavelength, so the graphene resonator can be regarded as dipole antenna.

The proposed metamaterial absorber can be regarded as a simple RLC resonance circuit [13]. Magnetic resonant frequency  $\omega_m$  of the entire structure can be expressed by  $\omega_m = 1/\sqrt{LC}$ , where  $L$  and  $C$  are the effective inductance and capacitance, respectively. Besides,  $L$  and  $C$  can be represented in qualitative ways [12,13,14] like  $L \propto (lt)/w$  and  $C \propto (wl/2)/t$ , where  $l$  is the length of graphene strips,  $t$  is the thickness of silicon layer and  $w$  is the width of graphene strips. Through the deducing of the formula, we get the qualitative  $\omega_m \propto 1/l$ . It is the reason why the range between the peaks is nearly the same for the different  $E_F$  as shown in Fig. 6.

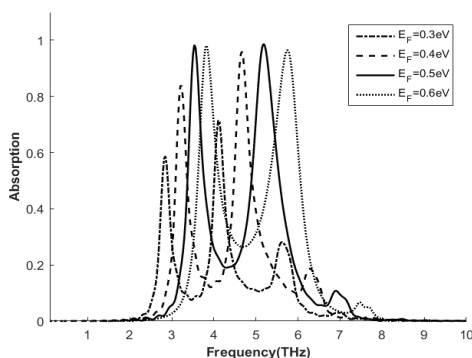


Fig. 6. The absorption spectra for different Fermi levels

## 5. Conclusions

This paper proposes a tunable dual band perfect graphene absorber in the range of THz. The structure shows a high absorption of 98.3% and 98.7% at 3.54THz and 5.12THz. It is easy to be fabricated and is insensitive to the polarization. The absorber has potential to develop highly sensitive and selective detectors in THz range.

## Acknowledgements

This research was supported in part by the National Natural Science Fund of China (Project number No. 61377075), the Youth Science Foundation Project of National Natural Science Foundation of China (Grant no. 61505144) and the Tianjin applied foundation and advanced technology research program (Youth Program No. 14JCQNJC00900).

## References

- [1] C. M. Watts, X. Liu, W. J. Padilla, *Advanced Materials* **24**(23), OP98 (2012).
- [2] Yanhan Z, Subash V, Yong Z, et al., *Opt. Lett.* **38**(14), 2382 (2013).
- [3] Z. Bo, H. Ting, S. Jingling, et al., *Opt. Lett.* **39**(21), 6110 (2014).
- [4] Y. Zhang, T. Li, B. Zeng, et al., *Nanoscale* **7**(29), 12682 (2015).
- [5] Y. Zhang, T. Li, C. Qi, et al., *Scientific Reports* **5** (2015).
- [6] Y. P. Zhang, T. T. Li, H. H. Lv, et al., *Chinese Physics Letters* **32**(6), (2015).
- [7] G. W. Hanson, *Journal of Applied Physics* **103**(6), 064302 (2008).
- [8] Run-Mei Gao, Zong-Cheng Xu, Chun-Feng Ding, et al., *Applied Optics* **55**(8), (2016).
- [9] Zhang, Longhui, Hu, Fangrong, Xu, Xinlong, et al., *Optics Communications* **369**, 65 (2016).
- [10] G. Yao, F. Ling, J. Yue, et al., *Opt. Express* **24**(2), (2016).
- [11] A. Andrei, A. V. Lavrinenko, *Opt. Express* **21**(7), 9144 (2013).
- [12] Y. Q. Ye, Y. Jin, S. He, *J. Opt. Soc. Am. B* **27**(3), 498 (2010).
- [13] Z. Jiangfeng, E. N. Economon, K. Thomas, et al., *Opt. Lett.* **31**(24), 3620-2 (2006).
- [14] Jiangfeng Zhou, Lei Zhang, Gary Tuttle, et al., *Physical Review B* **73**(4), (2006).

\*Corresponding author: letto1990@163.com; rgjl@163.com

\*\* six\_apple\_sword@163.com